JOURNAL OF COMPUTATIONAL PHYSICS 2, 126-153 (1967)

Dynamics of Nonlinear Lattices I. Localized Optical Excitations, Acoustic Radiation, and Strong Nonlinear Behavior[1]

NORMAN J. ZABUSKY AND GARY S. DEEM

Bell Telephone Laboratories, Incorporated, Whippany, New Jersey 07981

ABSTRACT

A one-dimensional lattice of equimass particles coupled to nearest neighbors by nonlinear "linear-plus-quadratic" force laws is excited with initial conditions for which alternate masses are displaced along *two* smooth curves. This results in an interaction between "acoustic," low-frequency motions and "optical," high-frequency motions. A continuum description in terms of a pair of coupled partial differential equations is introduced and analytical solutions obtained are found to agree quantitatively with small-amplitude, short-time, optical-acoustic interactions observed in *numerical* solutions of the lattice equations. Hence the lattice or discretization phenomenon known as "aliasing" (coupling of optical energies to acoustic energies) can be treated analytically by a continuum description if the energies involved are small. As the strength of the initial amplitudes is increased, this description in terms of two smooth curves becomes invalid, and "three-curve" states appear after a short time. A further increase in the nonlinearity results in a rapid cascade of energy across the entire modal energy spectrum. For the times considered, however, we fail to attain complete equipartition of the spectral energies. Instead, very regular features such as one-, two-, three-, and *higher*-curve states are observed to occupy a large fraction of the lattice length and are preserved as they propagate along and interact with each other.

I. INTRODUCTION

In this paper we consider a one-dimensional anharmonic lattice consisting of $N \gg 1$ discrete, equimass particles per unit interval interacting with nearest neighbors only, and whose Hamiltonian is

$$H = \tfrac{1}{2} \sum_{n=1}^{2N} [(\dot{y}_n/\omega)^2 + (y_n - y_{n-1})^2 + \tfrac{2}{3}\alpha(y_n - y_{n-1})^3]. \tag{1}$$

[1] Parts of this paper were presented at the International Congress of Mathematicians, Moscow, August 1966.

Here y_n denotes the displacement of particle n, $\omega^2 = \kappa/m$, κ is a "linear" spring constant, m is the constant mass of each particle, $\alpha > 0$ is a measure of the nonlinearity in the corresponding equations of motion, and a dot denotes time differentiation. We have restricted ourselves to a nonlinear interaction potential energy of the cubic type in (1) (that is, a linear-plus-quadratic force law), but the following approach is applicable to any lattice having short-range forces. This system provides a simple model for treating nonlinear wave propagation in discrete media such as solids [1] and plasmas [2–4]. In fact, we may think of the lattice as a discretized representation of a continuum and thus view some of the phenomena as resulting from discretization; that is, the response of the system to short wavelength excitations.

Of the wide class of motions available to the lattice, we distinguish between two basically different types, combinations of which can be excited by appropriate choice of the initial conditions $y_n(0), \dot{y}_n(0)$. By "acoustic" or low-frequency motions of the lattice, we denote time evolutionary situations in which all particle displacements y_n remain on a *single* smooth curve $y(x, t)$. "Optical" or high-frequency motions will be referred to when alternate particles move on *two* distinct, smooth curves $w(x, t)$ and $z(x, t)$. If we may assume that nonlinearities cause the optical states to interact only with the acoustic states (and we take N large), then we should be able to describe the lattice motion in terms of combinations of the two-curve states, w and z.

When the nonlinear forces are not too strong and in those cases where we impose fixed or periodic boundary conditions, another representation of the dynamics is given in terms of "linear" Fourier modal energies [5]. Acoustic motions [6, 7] then correspond to energy residing in the low frequency linear modes, and their basic property is wave propagation at the "sound speed" of the linear lattice. Optical motions correspond to energy in the highest frequency linear modes, and their basic property is high frequency vibration at the lattice frequency, ω/π. The modal representation, although well known to physicists, has rarely provided us with the basic understanding necessary for a proper analytical description of the dynamics. However, some of the results are summarized by presenting the modal energies vs time ("half" the information since the phase is omitted) because they do provide an alternate view of the dynamics.

Earlier treatments of similar lattices [8–14] have focused attention on long wavelength or acoustic excitations of this system, as first studied by Fermi, Pasta, and Ulam [5]. Solving initial value problems, starting with only the lowest linear mode, they observed that only the lowest linear modes of the lattice spectrum were excited. M. Kruskal and one of the authors succeeded in describing acoustic phenomena in terms of a continuum description of the lattice [1, 4]. In particular, for progressive waves on one characteristic, the Korteweg-de Vries equation, a third-order nonlinear partial differential equation, provides a long-time, uniform

asymptotic description of acoustic motions and predicts the near *recurrence* of sinusoidal initial states, which Fermi, Pasta, and Ulam observed for (1).

In the present paper we excite the optical modes of the lattice by a proper choice of initial conditions. In situations where random or well-mixed states of the lattice are present, optical excitations in the spectrum will be an important feature, so the present work is a prerequisite for an understanding of "turbulence" on the lattice. Furthermore, some heuristic work of Izrailev and Chirikov [15] suggests that for a lattice it may be easier to achieve mixing of energy, or a "stochastic" condition, when the energy resides initially in the high-frequency linear modes.

In Sec. II we treat optical-acoustic lattice motions in terms of a pair of partial differential equations, that is by a continuum description. The limitations of these equations to short times are discussed, and they are used to predict the generation of acoustic motions from purely optical initial conditions. In Sec. III a numerical solution of the lattice equations is discussed. It illustrates the generation and radiation of acoustic pulses from localized purely optical motions, and compares favorably with the analytical results of the continuum description of Sec. II. In Sec. IV the effect of increasing the relative size of nonlinear forces is described. We were surprised to find a qualitative departure from small nonlinear behavior—three-curve states were radiated by initial optical excitations. That is, in these states or packets the motion of every third particle is strongly correlated and, in effect, every third particle lies on a separate smooth curve. It is significant that for the times we consider, one finds a high degree of regularity in the motions y_n, as seen through a persistence of one-, two-, three-, and *higher*-curve states. The final example of Sec. IV illustrates this case. A generalization of the continuum methods for two-mass systems is given in Sec. V.

II. Continuum Description of Optical-Acoustic Excitations of an Anharmonic Lattice

The equations of motion of a lattice of particles whose Hamiltonian H is (1) can be written as

$$\omega^{-2}\ddot{y}_n = (y_{n+1} - 2y_n + y_{n-1})[1 + \alpha(y_{n+1} - y_{n-1})], \quad (n = 0, 1,..., 2N - 1). \tag{2}$$

Although we usually prescribe periodic boundary conditions ($y_{2N} = y_0$, etc.), this does not restrict the generality of our results as the periodic interval is larger than the initial length scales.

If we normalize the length of the periodic lattice to 2.0, then the particle spacing is

$$h = 1/N.$$

The dispersion relation for the "corresponding linear lattice" ($\alpha = 0$) (cf. Appendix I.A) is

$$\omega_k^2 = 4\omega^2 \sin^2\left(\frac{k\pi}{2N}\right), \qquad (k = 0, 1, \ldots, N), \tag{3}$$

and the mode $k = N$ corresponds to a vibration at the lattice frequency

$$\nu_0 = \frac{\omega_N}{2\pi} = \frac{\omega}{\pi}.$$

It is common to analyze systems like (2) through representations involving interacting normal modes. These are obtained by spatially Fourier decomposing y_n (Appendix I.B). In the study presented below we prefer to use a continuum representation of the various dynamical states that arise. However, it is sometimes convenient to view the state of a system by giving the energy in the spatial modes

$$H_k = H_k^L + H_k^{NL},$$

where H_k^L are the usually defined [5] "linear modal energies," H_k^{NL} are contributions from the nonlinear portion of (2), and $H = \sum_{k=0}^{N} H_k$ is a constant of the motion.

The optical portion of the lattice spectrum is excited if we displace particles alternately along two different smooth curves, as shown in Fig. 1. If we assume

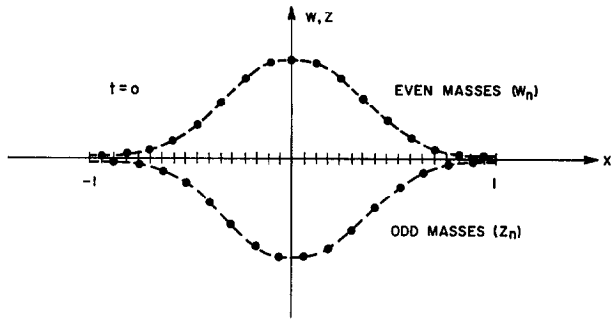

FIG. 1. Optical initial conditions.

that the particle displacements remain on two smooth curves at later times, the degrees of freedom available to the system are reduced, and one can easily obtain a continuum description in terms of these curves. This is a good assumption when the nonlinear interaction potential energy is cubic and a poor assumption when it is quartic. We will discuss the latter case at a future time.

If we distinguish between alternate masses, as we would, e.g., if they were different (as described in Sec. 5), we can write the equations of motion corresponding to (2) as

$$\begin{aligned} \omega^{-2}\ddot{w}_n &= (z_{n+1} - 2w_n + z_{n-1})[1 + \alpha(z_{n+1} - z_{n-1})], \qquad n = 0, 2, \ldots, 2N-2, \\ \omega^{-2}\ddot{z}_n &= (w_{n+1} - 2z_n + w_{n-1})[1 + \alpha(w_{n+1} - w_{n-1})], \quad n = 1, 2, \ldots, 2N-1. \end{aligned} \tag{4}$$

Here we denote the displacements y_n by w_n and z_n for even and odd masses, respectively. We assume that $w_n(t)$ and $z_n(t)$ are discrete approximations to a pair of sufficiently differentiable functions $w(x, t)$ and $z(x, t)$ on the interval $-1 \leqslant x < 1$, where $x = -1 + nh$. Denoting differentiation by ∂_x, ∂_t, etc., we may then write

$$w_{n\pm1} = w \pm h\partial_x w + \frac{h^2}{2!}\partial_x{}^2 w \pm \frac{h^3}{3!}\partial_x{}^3 w + \frac{h^4}{4!}\partial_x{}^4 w + O(h^4), \qquad n \text{ odd},$$

and similarly for $z_{n\pm1}$. We then find the following system for w and z:

$$\begin{aligned} \omega^{-2}\partial_t{}^2 w &= 2\left(1 + \epsilon\partial_x z + \frac{h^2}{6}\epsilon\partial_x{}^3 z\right)(z - w) + h^2(1 + \epsilon\partial_x z)\,\partial_x{}^2 z \\ &\quad + \frac{h^4}{12}\partial_x{}^4 z + O(\epsilon h^4), \\ \omega^{-2}\partial_t{}^2 z &= 2\left(1 + \epsilon\partial_x w + \frac{h^2}{6}\epsilon\partial_x{}^3 w\right)(w - z) + h^2(1 + \epsilon\partial_x w)\,\partial_x{}^2 w \\ &\quad + \frac{h^4}{12}\partial_x{}^4 w + O(\epsilon h^4), \end{aligned} \tag{5}$$

where $\epsilon = 2\alpha h$. If higher order terms do not contribute significantly to the equations of motion (5), then w and z are smooth curves, and these equations may give uniform descriptions of acoustic-optical lattice motions over long times. For example, if we consider only acoustical motions, then adjacent lattice points lie on the same smooth curve, or $w = z$, and (5) reduces to the acoustic equation studied in [1].

To separate the motions more effectively, we rewrite (5) in terms of average (acoustic) and difference (optical) variables

$$u(x, t) = \frac{w(x, t) + z(x, t)}{2}, \qquad v(x, t) = \frac{w(x, t) - z(x, t)}{2}$$

Adding and subtracting the equations in (5), we obtain

$$\omega^{-2}\partial_t^2 u = 4\epsilon v\partial_x\left(v + \frac{h^2}{6}\partial_x^2 v\right) + h^2\partial_x\left\{\partial_x u + \frac{\epsilon}{2}[(\partial_x u)^2 + (\partial_x v)^2]\right\} + \frac{h^4}{12}\partial_x^4 u + O(\epsilon h^4) \tag{6A}$$

$$\omega^{-2}\partial_t^2 v = -4v\left[1 + \epsilon\partial_x\left(u + \frac{h^2}{6}\partial_x^2 u\right)\right] - h^2\partial_x\{\partial_x v + \epsilon(\partial_x u)(\partial_x v)\} - \frac{h^4}{12}\partial_x^4 v + O(\epsilon h^4). \tag{6B}$$

In the present paper, we examine the coupling between acoustic and optical motions governed by (6) in the interesting "intermediate" regime where $\alpha = 1$, or

$$\epsilon = O(h),$$

that is, in terms of one dimensionless parameter. We restrict our investigation to times that are long with respect to optical time scales, $t_0 = 1/\nu_0$, but less than acoustic times, $t_A = 2/h\omega = 2/c$. (Here, t_A is the oscillation period for the lowest mode of the corresponding linear string, i.e., the lowest mode of the equation $\partial_t^2 u = c^2\partial_x^2 u$).

We assume a one-parameter ordering in which

$$u = \epsilon^m\tilde{u}, \qquad \partial_x u = \epsilon^{m+n}\partial_{x_1}\tilde{u}, \qquad \partial_t u = \epsilon^{m+r}\partial_{t_1}\tilde{u}$$

and

$$v = \epsilon^\mu\tilde{v}, \qquad \partial_x v = \epsilon^{\mu+\nu}\partial_{x_2}\tilde{v}, \qquad \partial_t v = \epsilon^{\mu+\rho}\partial_{t_2}\tilde{v},$$

where x_1, x_2, t_1 and t_2 are new independent variables chosen so that $\tilde{u}$, $\partial_{x_1}\tilde{u}$, etc., all have magnitudes at most $O(1)$. If we substitute these expressions into (6A) and (6B), omit constant multipliers, and treat $h = O(\epsilon)$, then the exponent ϵ in each term can be written as shown in Table I. A quick examination shows that

TABLE I

EXPONENTS OF ϵ IN EQUATION (6)

Term in (6)	1	2	3	4	5	6	7
A	$m+2r$	$1+2\mu+\nu$	$3+2\mu+3\nu$	$2+m+2n$	$3+2m+3n$	$3+2\mu+3\nu$	$4+m+4n$
B	$\mu+2\rho$	μ	$1+m+\mu+n$	$3+m+\mu+3n$	$2+\mu+2\nu$	$3+m+\mu+2n+\nu$ $3+m+\mu+n+2\nu$	$4+\mu+4\nu$

there are many possible orderings that are consistent. We ask whether there is a consistent ordering which agrees with the results of numerical computation, namely an ordering where terms 1 and 4 of (6A) compete and where terms 1 and 2 of (6B) compete.

Table II gives the relations one obtains when certain terms compete ($\equiv$) or are related by an inequality ($<$). Since $n > -1$, (f), then $r > 0$, a fact consistent

TABLE II

COMPETITION AMONG TERMS IN EQ. (6)

Competition			*Inequality*		
$A1 \equiv A4$:	$r = 1 + n$	(a)	$A3 < A2$; $A6 < A2$; $B5 < B2$:	$\nu > -1$	(d)
$A1 \leqq A2$:	$2r \leqslant 1 + 2\mu + \nu - m$	(b)	$A5 < A4$; $B3 < B2$:	$m + n > -1$	(e)
$B1 \equiv B2$:	$\rho = 0$	(c)	$A7 < A4$:	$n > -1$	(f)

with acoustic phenomena evolving more slowly than optical phenomena [$\rho = 0$, (c)]. Substituting (a) and (e) into (b), and assuming $\mu = m$ and $\nu = n$, we obtain

$$1 + n - m = 1 + \nu - \mu \leqslant 0.$$

We take $\nu = -\frac{1}{2}$ corresponding to a *localized* optical pulse and thus:

$$n = -\tfrac{1}{2}, \qquad r = \tfrac{1}{2}, \qquad \text{and} \qquad \mu \geqslant \tfrac{1}{2}.$$

Hence to order ϵ^2 (6) becomes

$$\begin{aligned}
\omega^{-2}\partial_{t_1}^2 \tilde{u} &= 4\epsilon^{\mu-1/2}\tilde{v}\partial_{x_1}\left(\tilde{v} + \epsilon\frac{\alpha^{-2}}{24}\partial_{x_1}^2\tilde{v}\right) \\
&\quad + \frac{\alpha^{-2}}{4}\partial_{x_1}\{\partial_{x_1}\tilde{u} + \tfrac{1}{2}\epsilon^{\mu+1/2}[(\partial_{x_1}\tilde{u})^2 + (\partial_{x_1}\tilde{v})^2]\} \\
&\quad + \epsilon\frac{\alpha^{-4}}{192}\partial_{x_1}^4\tilde{u} + O(\epsilon^2), \\
\omega^{-2}\partial_{t_1}^2\tilde{v} &= -4\tilde{v}(1 + \epsilon^{\mu+1/2}\partial_{x_1}\tilde{u}) - \epsilon\frac{\alpha^{-2}}{4}\partial_{x_1}^2\tilde{v} + O(\epsilon^2).
\end{aligned} \tag{7}$$

Normalizing the independent variables of (7)

$$\tau = 2\omega t, \qquad \xi = 2x/h,$$

we obtain

$$\partial_\tau^2 u_{(1)} - \partial_\xi^2 u_{(1)} = 2\alpha\partial_\xi(v_{(1)}^2), \tag{8A}$$

$$\partial_\tau^2 v_{(1)} + v_{(1)} = 0, \tag{8B}$$

where we use the original dependent variables u and v to first order. To this order the optical state drives the acoustic motion but there is no feedback from acoustic to optical.

We shall use (8) to predict quantitative features of the acoustic state u generated by initial conditions for which only a localized optical state v is nonzero, for example, the Gaussian displacement of v illustrated in Fig. 1 and given by

$$\begin{aligned} v(\xi, 0) &\equiv v_0(\xi) = \bar{v}\exp[-(h\xi/2\Delta)^2] \\ u(\xi, 0) &= u_\tau(\xi, 0) = v_\tau(\xi, 0) = 0. \end{aligned} \tag{9}$$

The parameter Δ, which determines the half-width of v in the original x coordinate, is typically taken as $O(h^{1/2})$ (localization). For short times, we may eliminate boundary considerations and assume an infinite line on which u and v decay exponentially at infinity. We will then be able to compare u and v with numerical solutions of Eq. (4) on the periodic lattice.

Equation (8A) is an inhomogeneous wave equation for $u_{(1)}$ in terms of $v_{(1)}$, and is easily inverted using the well known d'Alembert solution [16]

$$\begin{aligned} \partial_\xi u_{(1)}(\xi, \tau) &= F(\xi + \tau, \xi - \tau) \\ &\quad + \alpha\partial_\xi \int_0^\tau [v_{(1)}^2(\xi + \tau - \sigma, \sigma) - v_{(1)}^2(\xi - \tau + \sigma, \sigma)]\, d\sigma, \end{aligned} \tag{10}$$

where

$$F(\xi + \tau, \xi - \tau) = \tfrac{1}{2}[\partial_\xi u(\xi + \tau, 0) + \partial_\xi u(\xi - \tau, 0) + \partial_\tau u(\xi + \tau, 0) - \partial_\tau u(\xi - \tau, 0)].$$

We will be comparing analytically derived and numerically computed values of $\partial_\xi u$, because they allow a more severe comparison. We adopt our small parameter η as

$$\eta^2 \equiv \alpha^2 \max_\xi [v(\xi, 0)]^2 \ll 1. \tag{11}$$

It arises naturally if one assumes

$$2\epsilon\partial_x u \approx 4\alpha\partial_\xi u_{(1)} \ll 1,$$

and also if one takes the ratio of the nonlinear-to-linear energies in (1) and replaces the differences $y_n - y_{n-1}$ by $2v$. It is easily seen that the potential energy curve of adjacent oscillators gives rise to repulsive forces for values of η above 0.5. This

leads to exponentially increasing deviations or "runaway motions" of adjacent particles. We shall not consider such unphysical situations here.

For $\eta^2 \ll 1$, let us consider initial conditions where there are initial optical displacements and velocities

$$v(\xi, 0) = v_0(\xi), \qquad \partial_\tau v(\xi, 0) = \hat{v}_0(\xi),$$
$$F(\xi + \tau, \eta - \tau) = 0 \text{ (no initial acoustic state).} \tag{12}$$

The solution of (8B) is then

$$v_{(1)}(\xi, \tau) = v_0(\xi) \cos \tau + \hat{v}_0(\xi) \sin \tau,$$

corresponding to a linear lattice of independent harmonic oscillators. It follows from (10) that

$$\begin{aligned}\partial_\xi u_{(1)}(\xi, \tau) = \alpha\{&v_0^2(\xi + \tau) - 2[v_0(\xi) \cos \tau + \hat{v}_0(\xi) \sin \tau]^2 + v_0^2(\xi - \tau)\} \\ -\alpha \int_0^\tau \{&\sin 2\sigma\, [v_0^2(\xi + \tau - \sigma) + v_0^2(\xi - \tau + \sigma) \\ &- \hat{v}_0^2(\xi + \tau - \sigma) - \hat{v}_0^2(\xi - \tau + \sigma)] \\ &- 2 \cos 2\sigma\, [v_0(\xi + \tau - \sigma)\, \hat{v}_0(\xi + \tau - \sigma) \\ &+ v_0(\xi - \tau + \sigma)\, \hat{v}_0(\xi - \tau + \sigma)]\}\, d\sigma,\end{aligned} \tag{13}$$

where we have integrated by parts once.

In Appendix II we derive properties of (13) in several limiting cases. For example, if the initial conditions are given by (12) and if $v_0(\xi)$ and $\hat{v}_0(\xi)$ are sufficiently smooth, have extrema at $\xi = 0$, and if they tend to zero sufficiently rapidly as $|\xi|$ becomes large with respect to the width of the initial condition (the parameter $\beta \equiv 2\Delta/h \propto \epsilon^{-1/2}$), then

$$\partial_\xi u_{(1)}(\xi, \tau)\,|_{\xi=\tau} = \frac{\alpha}{2}\,[v_0^2(0) + \hat{v}_0^2(0)] + O\left(\frac{1}{\beta^2}\right), \tag{14}$$

when $\tau \gg \beta$, that is, long times. In Eq. (14), we follow that portion of the acoustic pulse at $\xi = \tau$ which moves with unit velocity from the origin, $\xi = 0$. Furthermore, assuming conditions on $v_0(\xi)$ and $\hat{v}_0(\xi)$ as above we also derive the form of the *nonpropagating* portion of (13) (which remains in any finite ξ-interval near $\xi = 0$ as $\tau \to \infty$) as

$$\partial_\xi u_{(1)}(\xi, \tau) \to \bar{u}'(\xi) + u_1'(\xi) \cos 2\tau + u_2'(\xi) \sin 2\tau, \tag{15}$$

where

$$\bar{u}'(\xi) = -\alpha[v_0^2(\xi) + \hat{v}_0^2(\xi)], \tag{16}$$

and

$$u_1'(\xi), u_2'(\xi) = O\left(\frac{1}{\beta^2}\right). \tag{17}$$

The acoustic state in (15) has a negligible oscillation about a mean value $\bar{u}'(\xi)$. The limit in (15) is uniform in any fixed, bounded ξ-interval.

III. Comparison of Analytical/Numerical Computations

A. Generation of Acoustic (One-Curve) States from Optical Initial Conditions, $\eta \ll 1$

To compare quantitatively the continuum formulation of Sec. II with numerical solutions of (4), we choose lattice initial conditions $w_n(0)$ and $z_n(0)$ for which there is no initial acoustic motion

$$\begin{aligned} w_n(0) &= \bar{v} \exp\left[-\left(\frac{n-N}{\Delta N}\right)^2\right], \qquad n \text{ even}, \\ z_n(0) &= -\bar{v} \exp\left[-\left(\frac{n-N}{\Delta N}\right)^2\right], \qquad n \text{ odd}, \\ \dot{w}_n(0) &= \dot{z}_n(0) = 0. \end{aligned} \tag{18}$$

We impose periodic boundary conditions, as usual. For the example of Fig. 2, $N = 200$, $\alpha = 1$, $\Delta = 0.106$, and $\bar{v} = 0.0175$, corresponding to a nonlinear strength

$$\eta = \alpha\bar{v} = 0.0175. \tag{19}$$

In the ordering scheme of the previous section, this corresponds to $\mu = 1$ in Eq. (7).

In Fig. 2 [first column, (a)] we have plotted at three different times the numerical differences for the w and z curves, namely

$$\begin{aligned} \delta_x w_n &\equiv \frac{w_{n+1} - w_{n-1}}{2h}, \qquad n = 1, 3, \ldots, 2N-3 \\ \delta_x z_n &\equiv \frac{z_{n+1} - z_{n-1}}{2h}, \qquad n = 2, 4, \ldots, 2N-2. \end{aligned} \tag{20}$$

For comparison, we have plotted in column (b) the corresponding average, or acoustic state $\partial_x \bar{u}(x, t)$, which is computed here by taking an average of the third-

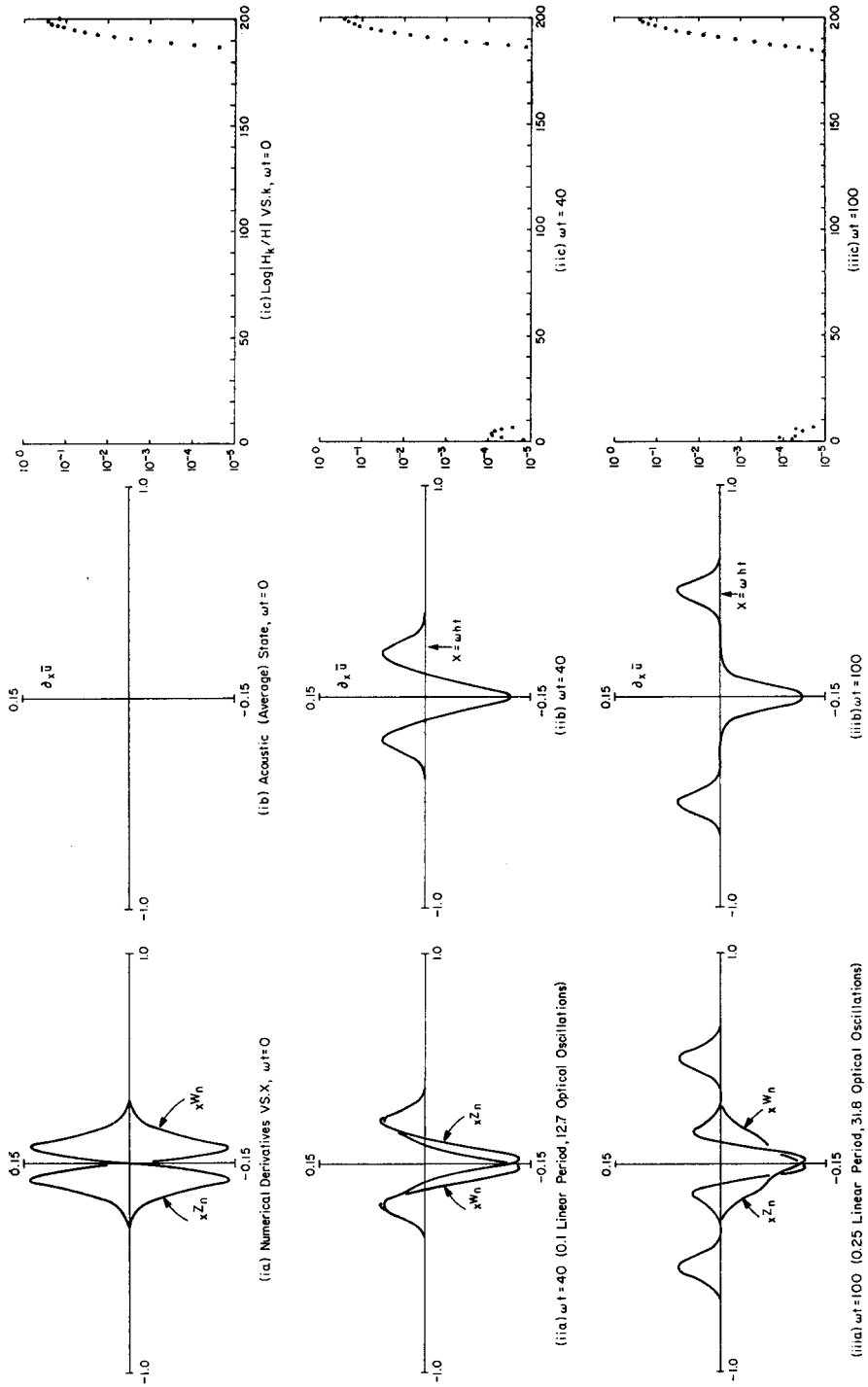

FIG. 2. Generation of an acoustic state from optical initial conditions ($\eta = 0.0175$, $N = 200$, $\Delta = 0.106$).

degree polynomials interpolated through four adjacent points of the $\delta_x w_n$ and $\delta_x z_n$ functions, respectively; that is

$$\partial_x \bar{u} \equiv \frac{1}{2} \begin{cases} \delta w_n + \frac{1}{16}[9(\delta z_{n+1} + \delta z_{n-1}) - (\delta z_{n+2} + \delta z_{n-2})], & n \text{ even} \\ \delta z_n + \frac{1}{16}[9(\delta w_{n+1} + \delta w_{n-1}) - (\delta w_{n+2} + \delta w_{n-2})], & n \text{ odd.} \end{cases} \tag{21}$$

In the presence of two-curve states only, (21) is a good approximation to the continuum function $\partial_x u$, with u as defined in the previous section. The last column of Fig. 2 gives logarithmic plots of the modal energies (defined in Appendix I.B). At $\omega t = 0$, we see that the excitation is confined to the high wavenumber modes. At $\omega t = 40$, we observe the formation of an acoustic state with a corresponding buildup in the low wavenumber energies.

At $\omega t = 100$, corresponding to 0.25 linear period (31.8 optical periods), two acoustic pulses have propagated away from the optical state, which then remains localized and vibrates nearly at the lattice frequency, ω/π. The ratio of the energy in the acoustic part of the spectrum to that in the optical part of the spectrum is $\alpha\bar{v}^2 = 3.06 \times 10^{-4}$. Except for a slow spreading of the optical state, this qualitative situation persists for two linear periods of 255 optical oscillations, that is, even when the propagating pulses return and interact with the central state (due to the periodic boundary conditions).

B. Comparison with the First-Order Continuum Description

For the initial conditions given in (18), the corresponding continuum initial conditions are

$$\begin{aligned} v(x, 0) &= \bar{v} \exp\left[-\left(\frac{x}{\Delta}\right)^2\right], \\ v_t(x, 0) &= u(x, 0) = u_t(x, 0) = 0. \end{aligned} \tag{22}$$

If $\beta = 2\Delta/h > 1$ and $\omega t \gg \beta$, we have from (14)

$$\partial_x u_{(1)}(x, t)\,|_{x=ct} = N\alpha\bar{v}^2\left[1 + O\left(\frac{1}{\beta^2}\right)\right] \approx 0.06125, \tag{23}$$

where we recall that $\xi = 2x/h = 2Nx$. This agrees with the height of the indicated pulse in (iiib) of Fig. 2 to within 0.25%, the approximate accuracy of the numerical calculations (Appendix III).

Furthermore, the value of $\partial_x u_{(1)}$ at the origin is given by (15–17) as

$$\partial_x u_{(1)}(x, t)\,|_{x=0} = -2N\alpha\bar{v}^2\left[1 + O\left(\frac{1}{\beta^2}\right)\right] \approx -0.1225. \tag{24}$$

In Fig. 3, we compare (13) (dashed line) with the numerical results for this case (solid line). Figure 4 gives the difference between Eq. (13) and $\partial_x \bar{u}$ (Fig. 2, iiib) at $\omega t = 100$ (0.25 of a linear period). The numerically computed minimum at the origin has risen to a 4.5% disagreement with (24), because of the continued interaction of the acoustic and optical state (which slowly spreads into the lattice).

If one allows *nonzero* initial optical velocities the results are essentially the same except that wave shapes are altered.

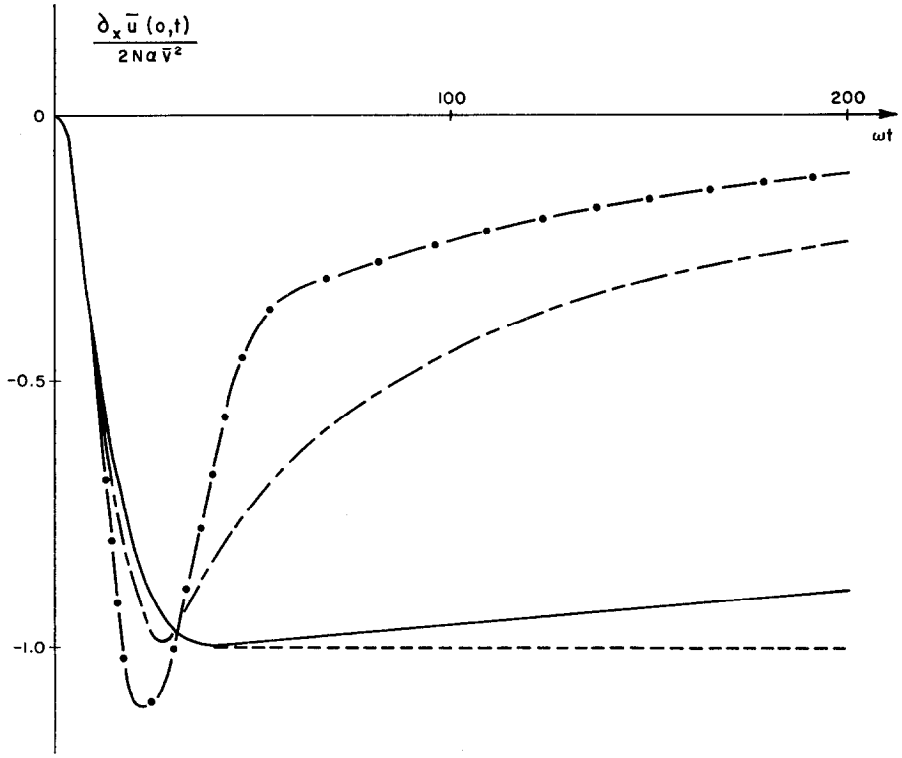

FIG. 3. Comparison of the acoustic states at $x = 0$, as derived from the continuum analysis (13) and from the numerical computations (21) ($N = 200$). – – – Eq. (13) ($\Delta = 0.106$); —— Eq. (21) ($\eta = 0.0175$, $\Delta = 0.106$); —·—·— Eq. (21) ($\eta = 0.163$, $\Delta = 0.1$); – · – Eq. (21) ($\eta = 0.326$, $\Delta = 0.1$).

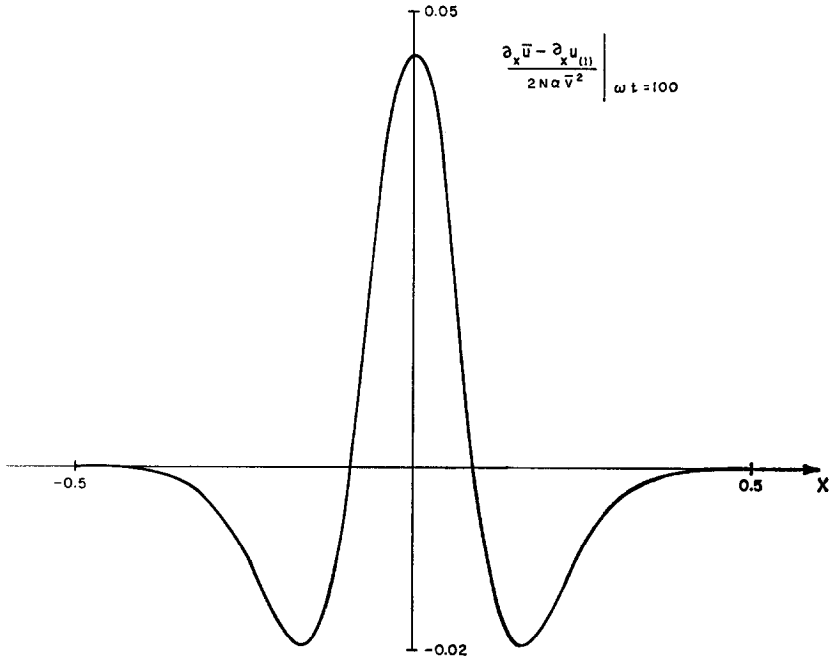

FIG. 4. The difference: $(\partial_x \bar{u} - \partial_x u_{(1)})/2N\alpha\bar{v}^2$ at $\omega t = 100$, as derived from (21) and (13) ($\eta = 0.0175$, $N = 200$, $\Delta = 0.106$).

IV. LARGE NONLINEAR EFFECTS; GENERATION OF "MULTI-CURVE" STATES [17]

The examples of the preceding section show that for values of η less than 0.1 a two-function continuum description can be used to describe the dynamics of a lattice with optical initial conditions for moderate time intervals. As η is increased beyond 0.1, we observe a qualitatively different lattice motion, namely, the presence of *three-curve* states. That is, every third particle of the lattice lies on a separate

[redacted]

three- and possibly higher-curve states.

The results of Fig. 5 are obtained with $\eta = 0.163$, $N = 200$, $\Delta = 0.1$ corresponding to $\mu = \frac{1}{2}$ in (7). We have plotted $\partial_x \bar{u}$ and observed that the two *radiated* acoustic pulses still have heights which are predicted by (23) to within about one percent, namely,

$$\partial_x \bar{u}(x, t) \Big|_{\substack{x=ct \\ \omega t=100}} = 5.37$$

and

$$\partial_x u_{(1)}(x, t)\,|_{\substack{x=ct \\ t\to\infty}} = 5.31 + O\left(\frac{1}{\beta^2}\right).$$

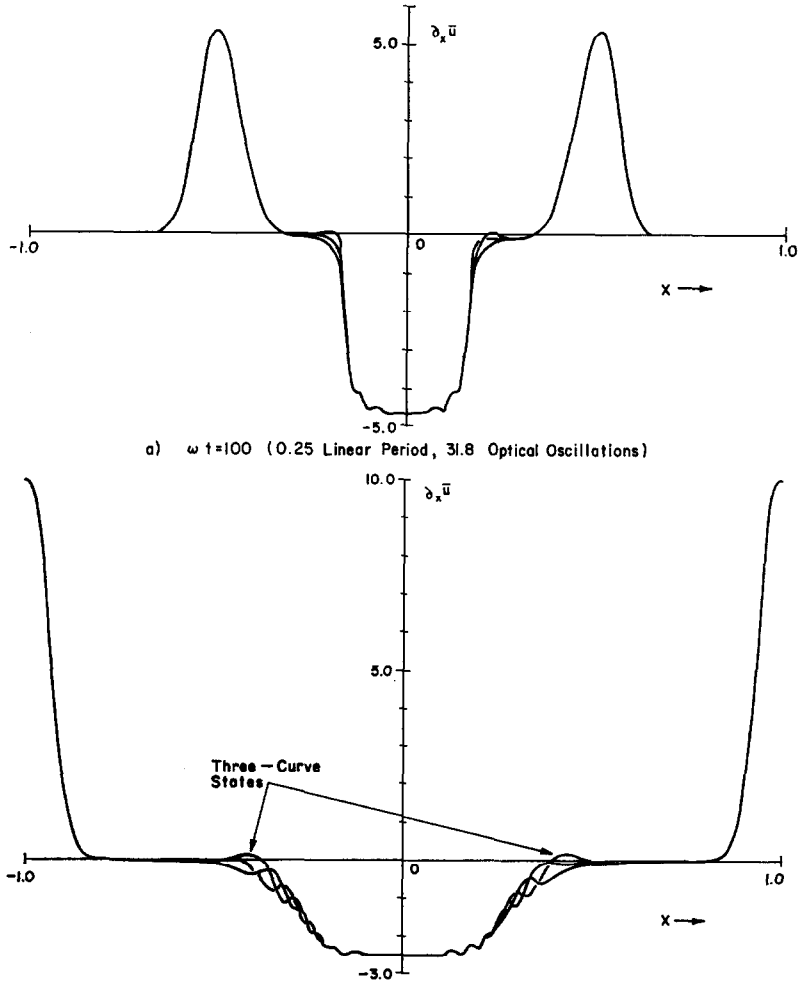

FIG. 5. Formation of three-curve states ($\eta = 0.163$, $N = 200$, $\Delta = 0.1$).

These radiated fronts are hardly affected by the deviation of the optical state from a simple harmonic oscillation. However the *central* acoustic state differs considerably from $\partial_x u_{(1)}$ after several oscillation periods t_0, as shown in Fig. 3, so that $v_{(1)}$ gives a valid approximation to v only for very short times. In Fig. 5a at $\omega t = 100$ (0.25 of a linear period), the minimum value of the acoustic state at $x = 0$ is less than 50% of that given by (24). In Fig. 5b at $\omega t = 200$ (0.5 of a linear period), the value of $\partial_x \bar{u}$ has fallen to 25% of (24) as a result of the "spreading" of the central region and the generation of three-curve states. These states propagate with a group velocity of approximately $c/2$, corresponding to a pulse whose mean wavenumber is $k = 2N/3$.

In Fig. 6 we have given plots of the modal energies. We note that for $\omega t = 100$, 0.310 of the total energy H resides in the midmodes, $k = 20$ to 180. [This compares

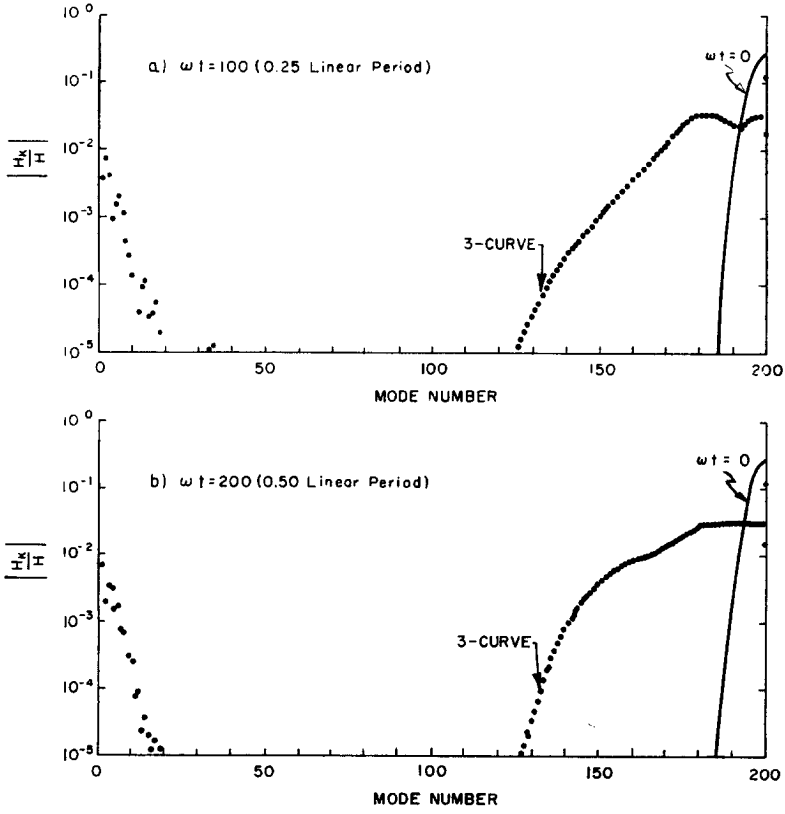

FIG. 6. Modal energy spectrum ($\eta = 0.163$, $N = 200$, $\Delta = 0.1$).

with 0.36×10^{-6} of H in the midmodes at $\omega t = 100$ for the $\eta = 0.0175$ case (Fig. 2)]. We also note that after $\omega t = 100$, the energy per mode remains less than 10^{-5} of H in the region $20 < k < 125$. Since an M-curve system will correspond to energy in modes centered about $k = 2N/M$, we therefore expect two- and three-function continuum descriptions to be adequate for describing lattice motions in the present case.

For our final example, we double the nonlinearity parameter to $\eta = 0.326$, keeping $N = 200$, $\Delta = 0.1$. The motion becomes much more complex in this case, consisting as usual of two propagating acoustic fronts which, however, do not separate from the oscillating central regions before encountering the boundaries, as they did in Fig. 5. In Fig. 7 we show $\partial_x \tilde{u}$, from (21), vs x at a time $\omega t = 200$ (0.5 of a linear period). The initial conditions are identical in form with those of the previous example, with their amplitudes doubled. We have produced a computer-generated film [17] for this case and have observed:

(a) In a very short time (a few optical oscillations t_0) the Max $|\, \delta_x w_n \,|$ and Max $|\, \delta_x z_n \,|$ grow considerably, but are quickly bounded as energy flows away from the central region via the acoustic fronts.

(b) The energy in the acoustic regions is sufficiently large, that one can see them steepen as they propagate away; that is, "shocks" are in the process of forming.

(c) In the spatial region between the acoustic and optical states, we see large amplitude three- and four-curve states. In Fig. 7, for the sake of clarity, we have drawn smooth curves through sets of points that have correlated motion. The three-curve states, for example, are observed to propagate with a velocity of approximately $c/2$.

(d) For times greater than half a linear period, when the periodic boundary effects give rise to more complicated motion, we still see many regions where there is correlated motion among groups of particles, including the four- and even five-curve states! Thus, the lattice does not seem to exhibit a truly random motion on these time scales.

This latter conclusion was somewhat contrary to our expectations, although it is analogous to the results of Fermi, Pasta, and Ulam [5] in the case of low amplitude, acoustic initial excitations. In Fig. 8 we show the evolution of the modal energies. At $\omega t = 0$ the energy resides in the highest optical modes; after 0.05 of a linear period (6.4 optical oscillations), Fig. 8a shows the rapid cascade of energy to the low end of the spectrum, together with a rising importance of many central modes. Very soon afterwards, we reach a state whose average features are exemplified by Fig. 8b (0.5 linear period). At this time 0.558 of H has been transferred to the central modes ($20 < k < 180$). At later times, one sees only small energy fluctuations about this nonuniform spectrum, indicating that our

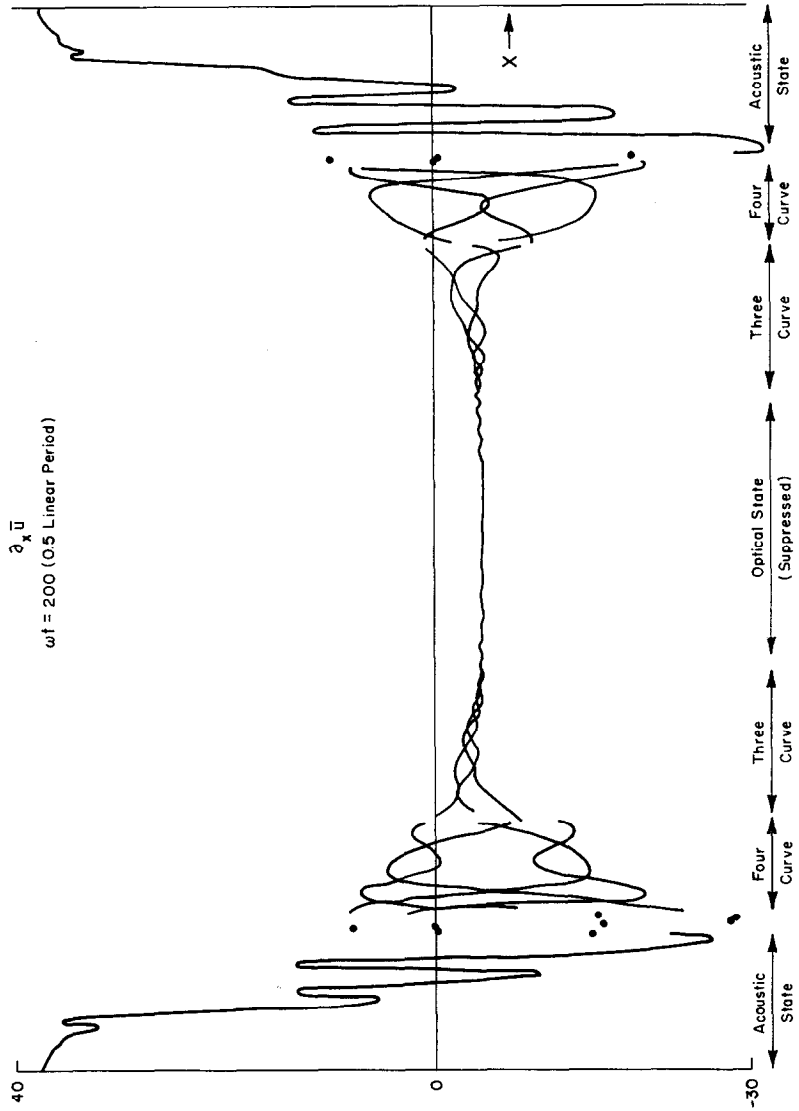

FIG. 7. Regular features in a strongly nonlinear example ($\eta = 0.326$, $N = 200$, $\Delta = 0.1$).

system does not reach a state of equilibrium having equipartition of energy among the various modes. This undoubtedly is due to the coherent states that we observe in Fig. 7. In Fig. 8b we have indicated those regions of the spectrum that would be occupied by one-, two-, three-, etc., curve states.

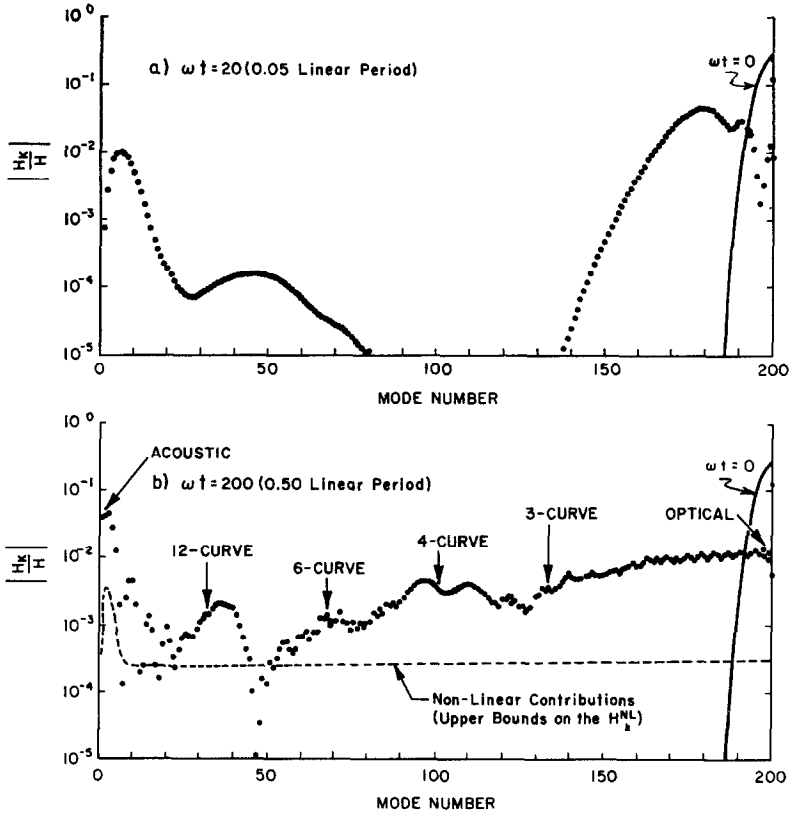

FIG. 8. Modal energies for strong nonlinear excitations ($\eta = 0.326$, $N = 200$, $\Delta = 0.1$).

In Fig. 8b we have also indicated a dotted line, below which fall the absolute values of all nonlinear contributions to the modal energies, according to our definitions of Appendix I.B. As can be seen, all but the least energetic modes agree to well within 10% of their linear modal energies H_k^L. Thus, the linear modal energies still give a qualitative measure of the state of excitation of each mode.

V. GENERALIZATIONS

Until now we have restricted ourselves to the specialized Hamiltonian (1), with corresponding equations of motion (2). We should emphasize that the continuum viewpoint for multifunction systems is applicable to more general

situations, for example, nonnearest-neighbor interactions and damping, i.e., velocity dependent terms, in (2).

We conclude with the generalization of (6) and (8) appropriate to a lattice for which even and odd particles have different masses m_1 and m_2, as for example in a crystal of sodium chloride. In this case the distinction between even and odd particle displacements is somewhat more natural than before; a two-curve description is needed, even in cases where the particles are initially displaced along a single smooth curve. We denote

$$\tilde{\omega}_1^2 = \kappa/m_1, \qquad \tilde{\omega}_2^2 = \kappa/m_2, \qquad \omega^2 = \tilde{\omega}_1\,\tilde{\omega}_2,$$
$$\sigma = \tilde{\omega}_2/\tilde{\omega}_1 = (m_1/m_2)^{1/2},$$

where κ again denotes the linear spring constant. Let $w(x, t)$ and $z(x, t)$ again denote continuum curves along which lie even and odd particle displacements $w_n(t)$ and $z_n(t)$, respectively. The equations of motion for w_n and z_n are similar to (4), except that we must replace ω^{-2} by $\tilde{\omega}_1^{-2}$ and $\tilde{\omega}_2^{-2}$ in the first and second of these equations, respectively.

In Appendix I.A we give the corresponding dispersion relation for the linearized lattice equations. The acoustic and optical branches are distinct, except in the case $\sigma = 1$, where (3) applies.

The generalization of (6) is found to be

$$\begin{aligned}\omega^{-2}\partial_t^2 u = {} & 4\mathfrak{F}_\sigma(u, v)\left[\frac{\sigma-1}{\sigma+1} + \epsilon\partial_x\left(v + \frac{h^2}{6}\,\partial_x^2 v\right)\right] \\ & + h^2\partial_x\left\{\partial_x u + \frac{\epsilon}{2}\left[\partial_x u \cdot \mathfrak{F}_\sigma(\partial_x v, \partial_x u) + \partial_x v \cdot \mathfrak{F}_\sigma(\partial_x u, \partial_x v)\right]\right\} \\ & + \frac{h^4}{12}\,\partial_x^4 u + O(\epsilon h^4), \end{aligned} \tag{25}$$

$$\begin{aligned}\omega^{-2}\partial_t^2 v = {} & -4\mathfrak{F}_\sigma(u, v)\left[1 + \epsilon\partial_x\left(u + \frac{h^2}{6}\,\partial_x^2 u\right)\right] \\ & - h^2\partial_x\left\{\partial_x v + \frac{\epsilon}{2}\left[\partial_x u \cdot \mathfrak{F}_\sigma(\partial_x u, \partial_x v) + \partial_x v \cdot \mathfrak{F}_\sigma(\partial_x v, \partial_x u)\right]\right\} \\ & - \frac{h^4}{12}\,\partial_x^4 v + O(\epsilon h^4), \end{aligned} \tag{26}$$

where

$$u = \frac{\tilde{\omega}_2 w + \tilde{\omega}_1 z}{\tilde{\omega}_2 + \tilde{\omega}_1}, \qquad v = \frac{\tilde{\omega}_2 w - \tilde{\omega}_1 z}{\tilde{\omega}_2 + \tilde{\omega}_1}$$

and

$$\mathfrak{F}_\sigma(f, g) = \frac{\sigma+1}{4}\left[\left(\frac{1}{\sigma} - 1\right)f + \left(\frac{1}{\sigma} + 1\right)g\right].$$

Corresponding to (8), we expect a short-time description of the optical-acoustic interactions to be given by

$$\begin{aligned} \partial_\tau^2 u_{(1)} - \partial_\xi^2 u_{(1)} &= \left(\frac{\sigma - 1}{\sigma + 1} + 4\alpha\partial_\xi v_{(1)}\right) \mathfrak{F}_\sigma(u_{(1)}, v_{(1)}) \\ \partial_\tau^2 v_{(1)} + \mathfrak{F}_\sigma(u_{(1)}, v_{(1)}) &= 0, \end{aligned} \tag{27}$$

where the ξ, τ coordinates are defined in (8). For example, (27) follows from the ordering hypotheses in Sec. II if we impose the additional requirement that

If $\sigma \neq 1$, we observe that the u motion is driven by an additional term $u_{(1)}\partial_\xi v_{(1)}$ and the u and v motions are coupled, even in the case $\alpha = 0$, and v is no longer harmonic. Thus, one might conjecture that there would be an increased tendency for the modal energies to relax toward a state of equipartition. This case warrants further study.

VI. Conclusions

We have shown that a two-function or two-curve continuum description can be used to describe analytically the dynamics of equimass, anharmonic lattices excited by weak, localized, optical initial states. As the strength of the excitation is increased, the two-curve description breaks down, and one sees multicurve states (in the numerical computations) radiated from regions containing one- and two-curve states. For very strong initial optical excitations, the multicurve states persist and the motion seems far from random.

These results are also indicative of the trouble that can arise in the numerical simulation of continuum phenomena. The process of discretizing a continuum is equivalent to setting up a lattice to represent the continuum. We observe that if nonlinear processes cause energy to flow to the high wavenumbers, then because of the discrete nature of the lattice this energy can be fed back to the low wavenumbers that we are in fact trying to simulate. This "aliasing" [18] error has been treated quantitatively in this paper for a one-dimensional problem when the optical energies are small.

VII. Acknowledgment

The authors would like to acknowledge valuable discussions with M. D. Kruskal of Princeton University.

APPENDIX I. DISPERSION RELATIONS AND SPECTRAL DECOMPOSITION

A. *Lattice Dispersion Relation*

Let us consider a one-dimensional chain of $2N$ particles, periodically extended, in which even particles have mass m_1 and displacement w_n and odd particles have mass m_2 and displacement z_n. The equations of motion are

$$\tilde{\omega}_1^{-2}\ddot{w}_n = z_{n+1} - 2w_n + z_{n-1}, \qquad n = 0, 2, \ldots, 2N-2,$$

$$\tilde{\omega}_2^{-2}\ddot{z}_n = w_{n+1} - 2z_n + w_{n-1}, \qquad n = 1, 3, \ldots, 2N-1,$$

where $\tilde{\omega}_1^2 = \kappa/m_1$, $\tilde{\omega}_2^2 = \kappa/m_2$ and κ is the spring constant. To determine the dispersion relation ω_k associated with mode k, set

$$w_{2n} = a_1 \exp\left[i\left(\frac{2nk\pi}{N} - \omega_k t\right)\right],$$

$$z_{2n+1} = a_2 \exp\left[i\left(\frac{(2n+1)k\pi}{N} - \omega_k t\right)\right]$$

for $n = 0, 1, \ldots, N-1$. We then find [7]

$$\omega_k^2 = \tilde{\omega}_1^2 + \tilde{\omega}_2^2 \pm \left(\tilde{\omega}_1^4 + \tilde{\omega}_2^4 + 2\tilde{\omega}_1^2\tilde{\omega}_2^2 \cos\frac{2k\pi}{N}\right)^{1/2}.$$

For the equimass systems to which we have restricted ourselves in this paper, $\tilde{\omega}_1^2 = \tilde{\omega}_2^2 = \omega^2$ and the above becomes

$$\omega_k^2 = 4\omega^2 \begin{Bmatrix} \sin^2 \dfrac{k\pi}{2N} \\ \cos^2 \dfrac{k\pi}{2N} \end{Bmatrix}, \qquad k = 0, 1, \ldots, \frac{N}{2}, \tag{28}$$

giving the acoustic, or low-frequency, branch and the optical, or high-frequency, branch respectively. In this case, the optical branch can be considered as an extension of the acoustic to $N/2 \leqslant k \leqslant N$. This convention was used for convenience in plotting the modal energy diagrams of Figs. 2, 5, 7 and 9 [e.g., $k = N$ in these diagrams actually corresponds to the $k = 0$ mode of the optical branch in (28)]. If $\tilde{\omega}_1 \neq \tilde{\omega}_2$ the optical and acoustic branches are separated by $2(\tilde{\omega}_1^2 - \tilde{\omega}_2^2)$ at $k = N/2$.

B. *Spectral Decomposition of Periodic Lattice Displacements and the Nonlinear Modal Energies*

To make precise our definition of "modal energies," especially for the nonlinear equimass Hamiltonian H in (1), we take a spatial spectral decomposition of $y_n(t)$

$$a_k(t) = \frac{1}{N^{1/2}} \sum_{l=0}^{2N-1} y_l(t) \sin \frac{lk\pi}{N},$$
$$b_k(t) = \frac{1}{N^{1/2}} \sum_{l=0}^{2N-1} y_l(t) \cos \frac{lk\pi}{N}, \qquad k = 0, 1, \ldots, N. \tag{29}$$

These can be inverted according to

$$y_n(t) = \frac{1}{N^{1/2}} \left\{ \frac{1}{2} [b_0 + (-1)^n b_N] + \sum_{k=1}^{N-1} \left(a_k \sin \frac{nk\pi}{N} + b_k \cos \frac{nk\pi}{N} \right) \right\}. \tag{30}$$

If we substitute (30) and its time derivative into (1) and rearrange terms, we find that

$$H = \sum_{k=0}^{N} (H_k^L + H_k^{NL}) \equiv \sum_{k=0}^{N} H_k, \tag{31}$$

where for $k = 1, \ldots, N-1$, $\omega_k = 2\omega \sin k\pi/2N$,

$$H_k^L = \frac{\omega^{-2}}{2} [(\dot{a}_k^2 + \dot{b}_k^2) + \omega_k^2 (a_k^2 + b_k^2)], \tag{32}$$

and

$$\begin{aligned} H_k^{NL} = {} & \frac{\alpha\omega^{-3}}{6(N)^{1/2}} \sum_{m=1}^{N-k} \{\omega_k\omega_m\omega_{k+m}[(a_k a_m - b_k b_m) a_{k+m} + (a_k b_m + b_k a_m) b_{k+m}] \\ & + 2\omega_k\omega_{N-m}\omega_{N-k-m}[(a_k a_{N-m} + b_k b_{N-m}) a_{N-k-m} \\ & + (a_k b_{N-m} - b_k a_{N-m}) b_{N-k-m}]\} \\ & + \frac{\alpha\omega^{-3}}{6(N)^{1/2}} \sum_{m=1}^{k} \{\omega_k\omega_{N-k+m}\omega_{N-m}[(a_k b_{N-k+m} + b_k a_{N-k+m}) b_{N-m} \\ & - (a_k a_{N-k+m} - b_k b_{N-k+m}) a_{N-m}]\}. \end{aligned} \tag{33}$$

For $k = 0$ and $k = N$

$$H_0^L = \frac{\omega^{-2}}{4} \dot{b}_0^2, \qquad H_N^L = \frac{\omega^{-2}}{4} (\dot{b}_N^2 + \omega_N^2 b_N^2), \qquad H_0^{NL} = 0,$$

and

$$H_N^{NL} = \frac{\alpha\omega^{-3}}{6(N)^{1/2}}\omega_N b_N \sum_{m=1}^{N-1} \omega_m \omega_{N-m}(b_m a_{N-m} + a_m b_{N-m}).$$

The choice (33) also preserves the property that

$$H_k = H_k{}^L = H_k^{NL} = 0, \qquad \text{if} \quad a_k = b_k = 0. \tag{34}$$

The energies H_k are no longer necessarily positive, nor indeed is the total energy H for all possible initial conditions.

The nonlinear contributions to the energies serve to couple the linear energies (32), so that except for $\alpha = 0$ they will no longer be constants of motion. Due to the lack of uniqueness in writing down (33), it is not very instructive to consider the energies H_k except in cases where they differ only slightly from their linear contributions $H_k{}^L$. For the examples of Sec. III, the ratio

$$\frac{|H_k^{NL}|}{|H_k|} \tag{35}$$

remains well below 1%, except for the very least excited modes. Even for the final (highly excited) case of Sec. IV, the ratio (35) eventually remains less than 10%, except for the least energetic modes.

The equations of motion (2) in modal form are written below for reference:

$$\begin{aligned} \ddot{a}_k + \omega_k{}^2 a_k &= -\alpha \sum_{m,n=1}^{N} (V_{kmn}^{(11)} a_m a_n + V_{kmn}^{(12)} a_m b_n + V_{kmn}^{(13)} b_m b_n) \\ \ddot{b}_k + \omega_k{}^2 b_k &= -\alpha \sum_{m,n=1}^{N} (V_{kmn}^{(21)} a_m a_n + V_{kmn}^{(22)} a_m b_n + V_{kmn}^{(23)} b_m b_n), \end{aligned} \tag{36}$$

where the $V_{kmn}^{(ij)}$ are polynomials in the ω_l. For example

$$\begin{aligned} V_{kmn}^{(11)} = {} & \frac{1}{2\omega(N)^{1/2}}\omega_k\omega_m\omega_n \\ & \cdot [(1 + \delta_{k,0})(\delta_{k,m+n} - \delta_{k,2N-m-n}) \\ & + (1 - \delta_{k,N})(\delta_{k,m-n} + \delta_{k,-m+n})] \\ \{V_{kNn}^{(11)} = V_{kmN}^{(11)} = V_{kNN}^{(11)} = 0\}, & \end{aligned}$$

for $1 \leqslant m, n \leqslant N - 1$ and $0 \leqslant k \leqslant N$. $\delta_{m,n}$ denotes the Kronecker delta.

Appendix II. Asymptotic Behavior of the Acoustic State for Large Times

Let $\varphi(\xi) = g(\xi/\beta)$, where β is a large parameter ($\beta \equiv 2\Delta/h \approx 40$ in the examples of Sec. III), and where g has two integrable derivatives and an absolutely integrable third derivative. Integration by parts then gives

$$\begin{aligned}\int_{\lambda}^{\infty} \varphi(\sigma)\, e^{2i\sigma} d\sigma &= \beta \int_{\lambda/\beta}^{\infty} g(\sigma)\, e^{2i\beta\sigma} d\sigma \\ &= \frac{i}{2} g\left(\frac{\lambda}{\beta}\right) e^{2i\lambda} - \frac{1}{4\beta} g'\left(\frac{\lambda}{\beta}\right) e^{2i\lambda} - \frac{1}{4\beta} \int_{\lambda/\beta}^{\infty} g''(\sigma)\, e^{2i\beta\sigma} d\sigma \\ &= \frac{i}{2} \varphi(\lambda)\, e^{2i\lambda} - \frac{1}{4} \varphi'(\lambda)\, e^{2i\lambda} + O\left(\frac{1}{\beta^2}\right), \end{aligned} \tag{37}$$

where a prime denotes differentiation with respect to the argument. The last line follows by noting that

$$\begin{aligned}\left| \int_{\lambda/\beta}^{\infty} g''(\sigma)\, e^{2i\beta\sigma} d\sigma \right| &= \left| -\frac{1}{2i\beta} g''\left(\frac{\lambda}{\beta}\right) - \frac{1}{2i\beta} \int_{\lambda/\beta}^{\infty} g'''(\sigma)\, e^{2i\beta\sigma} d\sigma \right| \\ &\leqslant \frac{1}{2\beta} \left[\max_{\xi} |\, g''(\xi)\,| + \int_{0}^{\infty} |\, g'''(\sigma)\,|\, d\sigma \right]. \end{aligned} \tag{38}$$

In order to examine the properties of $\partial_{\xi} u_{(1)}(\xi, \tau)$ for τ large, we write (13) as

$$\begin{aligned}\partial_{\xi} u_{(1)}(\xi, \tau) = \alpha \Big\{ & v_0^2(\xi + \tau) - 2[v_0(\xi) \cos \tau + \hat{v}_0(\xi) \sin \tau]^2 + v_0^2(\xi - \tau) \\ & - \sin 2(\xi + \tau) \int_{\xi}^{\xi+\tau} [(v_0^2(\sigma) - \hat{v}_0^2(\sigma)) \cos 2\sigma + 2 v_0(\sigma)\, \hat{v}_0(\sigma) \sin 2\sigma]\, d\sigma \\ & + \sin 2(\xi - \tau) \int_{\xi-\tau}^{\xi} [(v_0^2(\sigma) - \hat{v}_0^2(\sigma)) \cos 2\sigma - 2 v_0(\sigma)\, \hat{v}_0(\sigma) \sin 2\sigma]\, d\sigma \\ & + \cos 2(\xi + \tau) \int_{\xi}^{\xi+\tau} [(v_0^2(\sigma) - \hat{v}_0^2(\sigma)) \sin 2\sigma - 2 v_0(\sigma)\, \hat{v}_0(\sigma) \cos 2\sigma]\, d\sigma \\ & - \cos 2(\xi - \tau) \int_{\xi-\tau}^{\xi} [(v_0^2(\sigma) - \hat{v}_0^2(\sigma)) \sin 2\sigma + 2 v_0(\sigma)\, \hat{v}_0(\sigma) \cos 2\sigma]\, d\sigma \Big\}. \end{aligned} \tag{39}$$

Consider first the behavior of (39) at a point $\xi = \lambda + \tau$, where λ is held fixed; that is, we follow the acoustic pulse which originates at $\xi = \lambda$, as it moves toward

positive ξ at the "sound speed" of (8A). If $v_0^2(\xi) - \hat{v}_0^2(\xi)$ and $v_0(\xi)\,\hat{v}_0(\xi)$ satisfy the conditions on $\varphi(\xi)$ in (37), then as $\tau \to \infty$,

$$\begin{aligned}
&\partial_\xi u_{(1)}(\xi, \tau)|_{\xi=\lambda+\tau} \\
&\quad \to \alpha \Big\{ v_0^2(\lambda) + \sin 2\lambda \int_\lambda^\infty [(v_0^2(\sigma) - \hat{v}_0^2(\sigma)) \cos 2\sigma - 2v_0(\sigma)\,\hat{v}_0(\sigma) \sin 2\sigma]\, d\sigma \\
&\qquad - \cos 2\lambda \int_\lambda^\infty [(v_0^2(\sigma) - \hat{v}_0^2(\sigma)) \sin 2\sigma + 2v_0(\sigma)\,\hat{v}_0(\sigma) \cos 2\sigma]\, d\sigma \Big\} \\
&\quad = \frac{\alpha}{2} \{[v_0^2(\lambda) + \hat{v}_0^2(\lambda)] + [v_0(\lambda)\,\hat{v}_0(\lambda)]'\} + O\left(\frac{1}{\beta^2}\right),
\end{aligned} \tag{40}$$

uniformly in any fixed, bounded λ-interval. In particular, (14) follows if $v_0(\xi)$ and $\hat{v}_0(\xi)$ have extrema at $\xi = 0$.

Consider now the behavior at a fixed point ξ as $\tau \to \infty$. Let $v_0(\xi)$ and $\hat{v}_0(\xi)$ have properties as before. From (39) it is clear that as τ becomes large, $\partial_\xi u_{(1)}$ takes the form

$$\partial_\xi u_{(1)}(\xi, \tau) \to \bar{u}'(\xi) + u'_{(1)}(\xi) \cos 2\tau + u'_{(2)}(\xi) \sin 2\tau. \tag{41}$$

This limit is uniform in any fixed, bounded ξ-interval, where specifically

$$\bar{u}'(\xi) = -\alpha[v_0^2(\xi) + \hat{v}_0^2(\xi)], \tag{42}$$

$$u'_1(\xi) = \alpha[\mathfrak{F}_1(v_0^2 - \hat{v}_0^2\,;\, \xi) + 2\mathfrak{F}_2(v_0\hat{v}_0\,;\, \xi)], \tag{43}$$

$$u'_2(\xi) = \alpha[2\mathfrak{F}_1(v_0\hat{v}_0\,;\, \xi) - \mathfrak{F}_2(v_0^2 - \hat{v}_0^2;\, \xi)]. \tag{44}$$

Here we denote the functional forms

$$\mathfrak{F}_1(\varphi;\, \xi) \equiv \int_{-\infty}^\infty \varphi(\sigma) \sin 2(\xi - \sigma)\, d\sigma - \varphi(\xi) - 2\int_\xi^\infty \varphi(\sigma) \sin 2(\xi - \sigma)\, d\sigma,$$

$$\mathfrak{F}_2(\varphi;\, \xi) \equiv \int_{-\infty}^\infty \varphi(\sigma) \cos 2(\xi - \sigma)\, d\sigma.$$

From these representations (43) and (44) we have that the time oscillations in (41) are negligible, since u'_1 and u'_2 are both $O(\beta^{-2})$. For example,

$$\begin{aligned}
\mathfrak{F}_1(\varphi;\, \xi) &= \sin 2\xi \int_0^\infty [\varphi(\sigma) + \varphi(-\sigma)] \cos 2\sigma d\sigma \\
&\quad - \cos 2\xi \int_0^\infty [\varphi(\sigma) - \varphi(-\sigma)] \sin 2\sigma d\sigma - \varphi(\xi) \\
&\quad - 2 \sin 2\xi \int_\xi^\infty \varphi(\sigma) \cos 2\sigma d\sigma + 2 \cos 2\xi \int_\xi^\infty \varphi(\sigma) \sin 2\sigma d\sigma \\
&= O\left(\frac{1}{\beta^2}\right),
\end{aligned} \tag{45}$$

which follows after several applications of (37) with $\lambda = 0$ or ξ. A similar argument holds for $\mathfrak{F}_2(\varphi; \xi)$.

Appendix III. Numerical Procedure

The difference scheme used in Sec. III and IV in connection with (2) was

$$\dot{y}^{j+1} = \dot{y}_n{}^j + \omega^2 \cdot \Delta t(y_{n+1}^j - 2y_n{}^j + y_{n-1}^j)[1 + \alpha(y_{n+1}^j - y_{n-1}^j)]$$

$$y_n^{j+1} = y_n{}^j + \Delta t \cdot \dot{y}_n^{j+1}, \qquad n = 0, 1, \ldots, 2N - 1,$$

where Δt is the time increment in going from level j to level $j + 1$. Periodicity was always enforced at the boundaries:

$$y_{2N}^j = y_0{}^j, \qquad \text{etc.}$$

Since H is a conserved quantity for the exact Eq. (2), its evaluation from the above scheme serves as a check on the numerical integrity. In the examples of Figs. 2, 6 and 8, $\omega\Delta t$ was chosen small enough that the variations in H from its initial values never exceeded 0.25%. For this purpose it was necessary to use in excess of 785 time steps per natural oscillation period ν_0^{-1}. The example of Fig. 5 was somewhat less accurate; energy variations were as high as one percent. A typical calculation (with microfilm output) carried to 0.5 linear period using 400 particles ($N = 200$), takes 0.4 hour with the IBM 7094 computer.

References

1. N. J. Zabusky, "A Synergetic Approach to Problems of Nonlinear Dispersive Wave Propagation and Interaction," "Nonlinear Partial Differential Equations" (W. Ames, ed.). Academic Press, New York (1967).

Sciences, Report NYO 9082, May 1 (1960).
3. K. W. Morton, *Phys. Fluids* 7, 1800 (1964). Yu. A. Berezin and V. I. Karpman, *Zh. Eksperim. Teor. Fiz.* **51**, 1557 (1966). H. Washimi and T. Taniuti, *Phys. Rev. Letters* **17**, 996 (1966).
4. N. J. Zabusky and M. D. Kruskal, *Phys. Rev. Letters* **15**, 240 (1965).
5. E. Fermi, J. R. Pasta, and S. M. Ulam, "Collected Papers of E. Fermi," Vol. 2, p. 978. Univ. of Chicago Press, Chicago, Illinois (1965).
6. G. Leibfried, "Handbuch der Physik" (S. Flügge, ed.), Band VII, p. 168. Springer, Berlin (1955).
7. L. Brillouin, "Wave Propagation in Periodic Structures." McGraw-Hill, New York (1946).
8. S. M. Ulam, "A Collection of Mathematical Problems," Chap. 8, Sec. 8. Wiley (Interscience), New York (1960).

9. J. FORD, *J. Math. Phys. (N. Y.)* **2**, 787 (1961).
10. E. A. JACKSON, *J. Math. Phys. (N. Y.)* **4**, 686 (1963).
11. R. S. NORTHCOTE and R. B. POTTS, *J. Math. Phys. (N. Y.)* **5**, 383 (1964).
12. N. J. ZABUSKY, "Proceedings of the Conference of Mathematical Models in the Physical Sciences" (Stefan Drobot, ed.), p. 99. Prentice-Hall, Englewood Cliffs, New Jersey (1963).
13. N. J. ZABUSKY, *J. Math. Phys. (N. Y.)* **3**, 1028 (1962).
14. M. D. KRUSKAL and N. J. ZABUSKY, *J. Math. Phys. (N. Y.)* **5**, 231 (1964).
15. F. M. IZRAILEV and B. V. CHIRIKOV, *Soviet Phys. Doklady* **11**, 30 (1966).
16. P. GARABEDIAN, "Partial Differential Equations." Wiley, New York (1964).
17. See the motion picture "Formation, Propagation and Interaction of Solitons in Nonlinear Dispersive Media (Numerical Solutions of Differential Equations Describing Wave Motion in Nonlinear Dispersive Media)," by N. J. Zabusky, M. D. Kruskal and G. S. Deem, Bell Telephone Laboratories, Inc., Film Library, Murray Hill, New Jersey, 07971; Part III.
18. R. W. HAMMING, "Numerical Methods for Scientists and Engineers," p. 276. McGraw-Hill, New York (1962). Also see A. ARAKAWA, *J. Computational Phys.* **1**, 119 (1966).